Series-Connected Self-Excited Synchronous Generator: Steady State and Transient Behaviors

A.L. Mohamadein
BSc, MSc, PhD, MIEE, CEng and Sen MIEEE

H.A. Yousef
BSc, MSc, PhD and MIEEE

Y.G. Dessouky
BSc, MSc, PhD and MIEEE

Abstract: Series Connected Synchronous Generator (SCSG) is an induction machine with stator and rotor windings connected in series via excitation capacitors. This generator operates synchronously to produce sinusoidal output voltage with half rated frequency. This paper presents theoretical and experimental investigation for transient and steady state performances based on the d-q model as derived for a synchronously rotating frame. The minimum capacitor needed to cause self-excitation for a particular speed is calculated.

Keywords: Parameteric Machine, Induction Machine, Self Excitation, Synchronous Generator, Generalized Machine Theory

List of Symbols:

C	excitation capacitor, μF
C_{min}	minimum required capacitance for self excitation, μF
i_a, i_b, i_c	instantaneous currents in phases a, b and c respectively, A
i_{ar}, i_{br}, i_{cr}	instantaneous rotor currents in phases a, b and c respectively, A
i_{as}, i_{bs}, i_{cs}	instantaneous stator currents in phases a, b and c respectively, A
i_d, i_q	instantaneous currents in d and q axes coil respectively, A
i_{dr}, i_{ds}	instantaneous rotor and stator currents in d-axis coil respectively, A
i_{qr}, i_{qs}	instantaneous rotor and stator currents in q-axis coil respectively, A
I_d, I_q	steady state currents in (d) and (q) axes coil respectively, A
i_m	peak magnetization currents, A
I_L, I_a	rms steady state load and armature currents per phase respectively, A
K	effective rotor to stator turns ratio
l_s, l_r	stator and rotor leakage inductance respectively, H
L_s, L_r	stator and rotor self inductances respectively, H
L_d, L_q	self inductances of (d) and (q) axes respectively, H
M	maximum mutual inductance between rotor and stator, H
N	rotor speed, rpm
P	differential operator
R_s, R_r	stator and rotor resistance respectively, Ω
R_L, L	load resistance (Ω) and inductance (H) respectively.
v_a, v_b, v_c	instantaneous voltage of phase a, b and c respectively, V
v_d, v_q	instantaneous voltages of d and q axes coil respectively, V
V_d, V_q	steady state voltages of d and q axes coils respectively, V
V_a	rms steady state voltage per phase, V
X_s, X_r	stator and rotor leakage reactance at base frequency, Ω
Z_{Le}	equivalent impedance of the inductive load and excitation capacitor parallel combination, Ω
ω_e, ω	MMFs and rotor speeds respectively, rad/s

I. INTRODUCTION

Interest in renewable energy systems has recently increased due to increase in energy consumption rate. Therefore research work has been lately devoted to explore the different types of renewable energies.

Self-excited induction generator is suitable for converting wind energy into electric type since it can operate over a wide range of speed. Performance study of self-excited induction generator [1]-[4] showed that the output voltage has a load dependent frequency.

Series Connected Synchronous Generator (SCSG) was proposed to produce sinusoidal output voltage whose frequency is dependent only on speed. SCSG is a slip ring induction machine whose stator and rotor windings are connected in series with sequence of two phases reversed as shown in Fig. 1. As a result, stator and rotor MMFs will rotate at the same speed (ω_e) but in opposite directions. Self-excitation process commences with the same manner as in self-excited induction generator using excitation capacitors. With reference to Fig. 2, electro-mechanical energy conversion is possible only when stator and rotor MMFs rotate synchronously at an absolute speed (ω_e) equal to half rotor speed (ω). SCSG has been analyzed using Floquet theory for solving resulting differential equations with time varying coefficients [5]-[6]. The analysis presented could not account for the effect of individual machine parameters. Another approach was presented in [7] to examine the effects of these parameters based on a deduced phase diagram. It was concluded that stator/rotor turns ratio plays major role in defining machine performance. However this approach needs iterations and is limited to predict steady-state performance only.

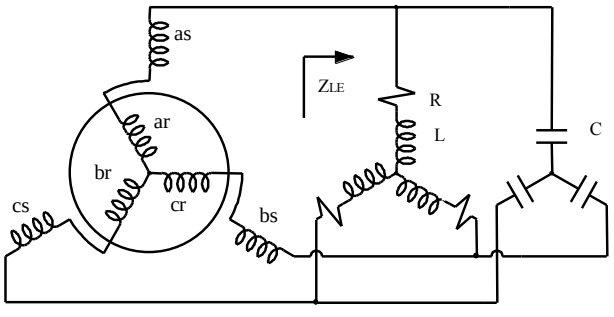

Fig 1. Schematic diagram for SCSG

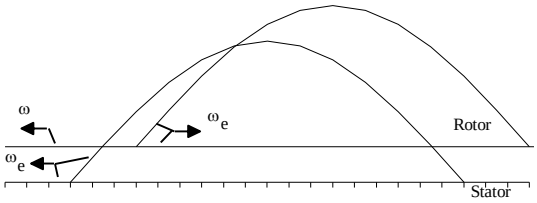

Fig. 2 MMF for stator and rotor in SCSG

In the present paper, the machine is analyzed using generalized theory of electrical machines. The approach based on d-q model is suitable for predicting both transient and steady-state performances. The minimum capacitor value to cause self-excitation for a particular speed is calculated.

II. D-Q MODEL REPRESENTATION

A. Machine representation

To analyze this generator, a reference frame rotates synchronously with stator and rotor MMFs was chosen. Since the rotor actually rotates with double reference frame speed, and with reference to Fig. 3, the following relation holds for every rotor position.

$$\theta = \beta \tag{1}$$

Reversing stator and rotor phase sequence windings can be expressed mathematically by:

$$\begin{bmatrix} i_{ar} \\ i_{br} \\ i_{cr} \end{bmatrix} = \begin{bmatrix} i_{as} \\ i_{cs} \\ i_{bs} \end{bmatrix} \tag{2}$$

Equivalent stator and rotor d-q currents in terms of actual phase currents and mutual displacements are given by the well known transformations [8].

$$\begin{bmatrix} i_{dr} \\ i_{qr} \end{bmatrix} = \frac{2}{3} \begin{bmatrix} \cos(\beta) & \cos\left(\beta + \frac{2\pi}{3}\right) & \cos\left(\beta - \frac{2\pi}{3}\right) \\ -\sin(\beta) & -\sin\left(\beta + \frac{2\pi}{3}\right) & -\sin\left(\beta - \frac{2\pi}{3}\right) \end{bmatrix} \begin{bmatrix} i_{ar} \\ i_{br} \\ i_{cr} \end{bmatrix} \tag{3}$$

and,

$$\begin{bmatrix} i_{ds} \\ i_{qs} \end{bmatrix} = \frac{2}{3} \begin{bmatrix} \cos(\theta) & \cos\left(\theta - \frac{2\pi}{3}\right) & \cos\left(\theta + \frac{2\pi}{3}\right) \\ \sin(\theta) & \sin\left(\theta - \frac{2\pi}{3}\right) & \sin\left(\theta + \frac{2\pi}{3}\right) \end{bmatrix} \begin{bmatrix} i_{as} \\ i_{bs} \\ i_{cs} \end{bmatrix} \tag{4}$$

Substituting by (1) and (2) into (3) and comparing the result with (4) yields:

$$\begin{Bmatrix} i_{ds} = i_{dr} = i_d \\ i_{qs} = -i_{qr} = i_q \end{Bmatrix} \tag{5}$$

Implementing the conditions derived in (5) to the d-q model results in the interconnections between axes equivalent coils shown in Fig. 4. It is seen that:

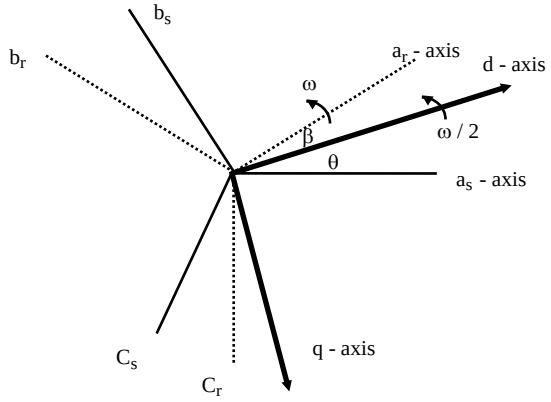

Fig. 3 Axes of 2-pole, 3-phase symmetrical induction motor

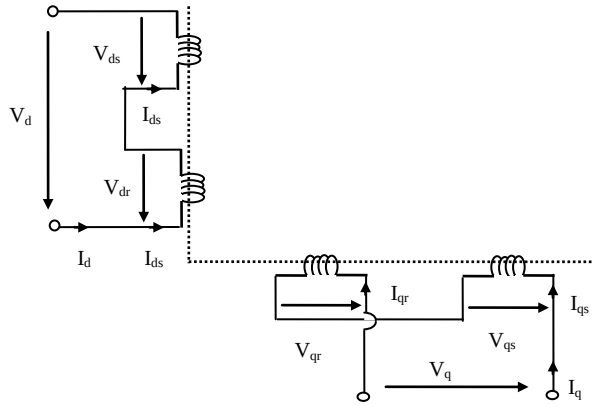

Fig. 4 Basic d-q circuit model of SCSG

$$\begin{Bmatrix} v_d = v_{ds} + v_{dr} \\ v_q = v_{qs} - v_{qr} \end{Bmatrix} \tag{6}$$

The relation between d-q axes voltages and currents can be expressed as:

$$\begin{bmatrix} v_d \\ v_q \end{bmatrix} = \begin{bmatrix} R + L_d P & L_q P\theta \\ -L_d P\theta & R + L_q P \end{bmatrix} \begin{bmatrix} i_d \\ i_q \end{bmatrix} \tag{7}$$

where,

$$\begin{Bmatrix} R = R_s + R_r \\ L_d = L_s + L_r + 2M \\ L_q = L_s + L_r - 2M \end{Bmatrix} \tag{8}$$

The series connection between stator and rotor phase windings resulted in effective saliency as indicated by difference in axes inductances which suggests synchronous operation of this machine.

B. Saturation representation

To take saturation in the iron parts into account, L_d and L_q are represented as a function of i_d and i_q as follows.
(i_m) is related to d-q currents by:

$$i_m = \sqrt{\left(i_{ds} + Ki_{dr}\right)^2 + \left(i_{qs} + Ki_{qr}\right)^2} \tag{9}$$

Substituting by (5) into (9) yields:

$$i_m = \sqrt{(1+K)^2\, i_d^2 + (1-K)^2\, i_q^2} \qquad (10)$$

From open circuit test, the relationship between the RMS air gap voltage V_g and magnetization current I_μ is evaluated. For each point, M and i_m are calculated as:

$M = Vg/(\omega * I_\mu)$ and $i_m = 1.41 * I_\mu$

The relationship between M and i_m shown in Fig. 5 can be expressed mathematically by a polynomial of the third order. The coefficients of that polynomial are concluded from Fig. 5 as given in section (III). Self inductances are related to leakage and mutual inductances by:

$$\left.\begin{aligned} L_s &= l_s + KM \\ L_r &= l_r + KM \end{aligned}\right\} \qquad (11)$$

Substituting by (11) into (8) and rearranging results in:

$$\left.\begin{aligned} L_d &= K_o + K_1 M \\ L_q &= K_o + K_2 M \end{aligned}\right\} \qquad (12)$$

where,

$$\left.\begin{aligned} K_o &= l_s + l_r \\ K_1 &= K + \frac{1}{K} + 2 \\ K_2 &= K_1 - 4 \end{aligned}\right\} \qquad (13)$$

It should be noted that because M is changing, an additional term (i_m PM) needs to be included in the voltage equations. However, with numerical methods implementation, M is assumed constant at each integration step.

C. Load representation

Self-excitation of SCSG is achieved by a capacitor bank to provide the leading reactive power required. The load is connected in parallel with excitation capacitors as shown in Fig. 1. Representing load and excitation circuits using d-q transformations is detailed in Appendix (A). The transient equations relating d-q voltages and currents are given by:

$$\left(1 - \frac{\omega^2 LC}{4}\right)\begin{bmatrix} v_d \\ v_q \end{bmatrix} + \left(R_L \frac{\omega}{2} C + LC\frac{P\omega}{2}\right)\begin{bmatrix} v_q \\ -v_d \end{bmatrix}$$
$$+ R_L C\begin{bmatrix} Pv_d \\ Pv_q \end{bmatrix} + \omega LC\begin{bmatrix} Pv_q \\ -Pv_d \end{bmatrix} + LC\begin{bmatrix} P^2 v_d \\ P^2 v_q \end{bmatrix} = \qquad (14)$$
$$-R_L\begin{bmatrix} i_d \\ i_q \end{bmatrix} - \frac{\omega L}{2}\begin{bmatrix} i_q \\ -i_d \end{bmatrix} - L\begin{bmatrix} Pi_d \\ Pi_q \end{bmatrix}$$

For resistive load, substitute (L) by zero in (14) and rearranging to get:

$$\frac{1}{R_L C}\begin{bmatrix} v_d \\ v_q \end{bmatrix} + \frac{\omega}{2}\begin{bmatrix} v_q \\ -v_d \end{bmatrix} + \begin{bmatrix} Pv_d \\ Pv_q \end{bmatrix} = -\frac{1}{C}\begin{bmatrix} i_d \\ i_q \end{bmatrix} \qquad (15)$$

To represent SCSG at no-load, (R_L) is substituted by infinity in (15) which yields:

$$\frac{\omega}{2}\begin{bmatrix} v_q \\ -v_d \end{bmatrix} + \begin{bmatrix} Pv_d \\ Pv_q \end{bmatrix} = -\frac{1}{C}\begin{bmatrix} i_d \\ i_q \end{bmatrix} \qquad (16)$$

So (14), (15) and (16) represent inductive, resistive and no-load cases respectively.

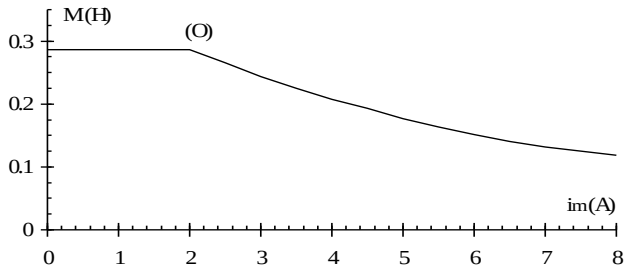

Fig. 5 Mutual inductance and magnetization current relationship

III. EXPERIMENTAL SETUP

The experimental setup is made from a slip ring, three phase induction machine whose details are: 220/380V, 6.3/3.6A, 2.2kW, 50Hz, 1390rpm. The parameters as has been obtained by standard tests at 50 Hz are as follows.

R_s=2.08Ω, R_r=1.96Ω, X_s=5.28Ω, X_r=3.92Ω and K=0.86.

The relation between M and i_m is depicted by Fig. 5 which when fitted results in,

$$M = \begin{cases} 0.286 & i_m < 2 \\ 0.4 - 0.067 i_m + 0.005 i_m^2 - 0.00015 i_m^3 & i_m \geq 2 \end{cases} \qquad (17)$$

The induction machine is connected in the SCSG mode as shown in Fig. 1 and mechanically coupled to a separately excited dc motor.

IV. TRANSIENT ANALYSIS

Voltage building up in this generator is a transient phenomena and it takes place by residual magnetism presented in iron. Dynamic model at no-load is introduced to predict voltage pattern during building up. Machine and no-load representation of (7) and (16) respectively can be rearranged as follows:

$$\begin{bmatrix} Pi_d \\ Pi_q \\ Pv_d \\ Pv_q \end{bmatrix} = \begin{bmatrix} \frac{-R}{L_d} & \frac{-\omega L_q}{2L_d} & \frac{1}{L_d} & 0 \\ \frac{\omega L_d}{2L_q} & \frac{-R}{L_q} & 0 & \frac{1}{L_q} \\ \frac{-1}{C} & 0 & 0 & \frac{-\omega}{2} \\ 0 & \frac{-1}{C} & \frac{\omega}{2} & 0 \end{bmatrix}\begin{bmatrix} i_d \\ i_q \\ v_d \\ v_q \end{bmatrix} \qquad (18)$$

Using Euler time stepping numerical techniques to solve (18), the transient behavior is obtained for each speed and capacitor as follows:

1. initial values are assigned for v_q, v_d, i_d and i_q to represent residual magnetization and time is set to zero.
2. (i_m), (M) and (L_d & L_q) are calculated from (10), (17) and (12) respectively.
3. Pi_d, Pi_q, Pv_d and Pv_q are evaluated from (18).
4. time, d-q currents and voltages are updated for next time step.
5. voltage of phase (a) is given by:

$$v_a = v_d \cos\left(\frac{\omega t}{2}\right) + v_q \sin\left(\frac{\omega t}{2}\right) \qquad (19)$$

Steps (2) to (5) are repeated until phase voltage reaches steady state. Predicted and experimental voltage building up are shown in the parts of Fig. 6.

(a)

(b)

Fig. 6 (a) Theoretical (b) experimental voltage waveform
N =1500 rpm and C = 110 μF (200V/div and 0.5 ms /div)

IT should be noted that agreement between theoretical and experimental results especially in the transient regime greatly depends on the assumption of initial conditions of voltages and currents.

V. STEADY STATE ANALYSIS

A. Steady state analysis for resistive load

The d-q model can also be used to analyze steady state at which:

$$Pi_d = Pi_q = Pv_d = Pv_q = 0 \tag{20}$$

Substituting by (20) into (7) and (15) and rearranging yields:

$$\begin{bmatrix} 1 & 0 & -R & \frac{L_d\omega}{2} \\ 0 & 1 & \frac{-L_q\omega}{2} & -R \\ \frac{\omega}{2} & \frac{1}{R_L C} & 0 & \frac{1}{C} \\ \frac{-1}{R_L C} & \frac{\omega}{2} & \frac{-1}{C} & 0 \end{bmatrix} \begin{bmatrix} V_q \\ V_d \\ I_q \\ I_d \end{bmatrix} = 0 \tag{21}$$

At steady state, neither (V_d), (V_q), (I_d) nor (I_q) equals zero. Therefore, the determinate of the 4×4 matrix of (21) should equal zero. This results in:

$$\left(\frac{\omega^4}{16} + \frac{\omega^2}{4R_L^2C^2}\right) L_qL_d - \frac{\omega^2}{4C}\,(L_q + L_d) + \left(\frac{R^2}{R_L^2C^2} + \frac{R^2\omega^2}{4} + \frac{1}{C^2} + \frac{2R}{R_LC^2}\right) = 0 \tag{22}$$

Substituting by (12) into (22) to get:

$$a_oM^2 + b_oM + c_o = 0 \tag{23}$$

Solving (23), M can then be given by:

$$M = \frac{-b_o - \sqrt{b_o^2 - 4a_o\,c_o}}{2a_o} \tag{24}$$

where,

$$\left\{\begin{aligned} a_o &= K_1K_2\left(\frac{\omega^4}{16} + \frac{\omega^2}{4R_L^2C^2}\right) \\ b_o &= (K_1 + K_2)\left(K_o\left(\frac{\omega^4}{16} + \frac{\omega^2}{4R_L^2C^2}\right) - \frac{\omega^2}{4C}\right) \\ c_o &= K_o^2\left(\frac{\omega^4}{16} + \frac{\omega^2}{4R_L^2C^2}\right) - \frac{K_o\omega^2}{2C} \\ &\quad + \left(\frac{R^2}{R_L^2C^2} + \frac{R^2\omega^2}{4} + \frac{1}{C^2} + \frac{2R}{R_LC^2}\right) \end{aligned}\right\} \tag{25}$$

Using curve fitting techniques to the magnetization curve (Fig. 5) to express i_m mathematically as a function of M results in:

$$i_m = 55.37 - 1035.94M + 9328.92M^2 - 44202M^3 + 101425M^4 - 68410.8M^5 - 62471.2M^6 \tag{26}$$

With reference to (21), (I_q) can be expressed as a function of (I_d) as follows:

$$I_q = h\,I_d \tag{27}$$

where,

$$h = \frac{-\frac{1}{C} - \frac{R}{R_LC} + \frac{L_d\omega^2}{4}}{\frac{\omega R}{2} + \frac{L_q\omega}{2R_LC}} \tag{28}$$

Substituting by (27) in (10) and rearranging results in:

$$I_d = \frac{i_m}{\sqrt{(1+K)^2 + (1-K)^2h^2}} \tag{29}$$

Then from (21),

$$\left\{\begin{aligned} V_q &= RI_q - L_dI_d\frac{\omega}{2} \\ V_d &= RI_d + L_qI_q\frac{\omega}{2} \end{aligned}\right\} \tag{30}$$

So for each speed, capacitor and load resistor, M and the corresponding i_m are calculated from (24) and (26) respectively. Also (h), (I_d), (I_q), (V_q) and (V_d) are calculated as given in (27) to (30). Finally:

$$\left\{\begin{array}{ll} V_a = \sqrt{\dfrac{V_d^2 + V_q^2}{2}}, & I_a = \sqrt{\dfrac{I_d^2 + I_q^2}{2}} \\ I_L = \dfrac{V_a}{R_L}, & \text{Output Power} = 3V_aI_L \end{array}\right\} \qquad (31)$$

Predicted and measured results are shown in Fig. 7.

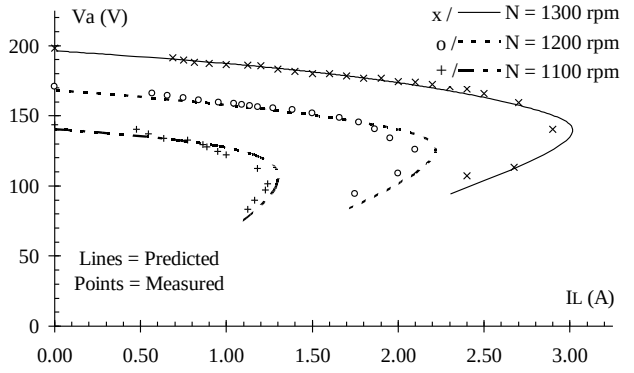

Fig. 7 Phase voltage and current relationship for resistive load (C=80μF)

B. Steady state analysis at no-load

Same procedure followed in section A for resistive load is used to evaluate performance on no-load by substituting (R_L) by infinity into (25) and (28) which tend to:

$$\left\{\begin{array}{l} a_o = K_1K_2\dfrac{\omega^4}{16} \\ b_o = (K_1+K_2)\left(K_o\dfrac{\omega^4}{16} - \dfrac{\omega^2}{4C}\right) \\ c_o = \dfrac{K_o^2\omega^4}{16} - \dfrac{K_o\omega^2}{2C} + \dfrac{R^2\omega^2}{4} + \dfrac{1}{C^2} \end{array}\right\} \qquad (32)$$

and,

$$h = \frac{\omega^2 CL_d - 4}{2RC\omega} \qquad (33)1$$

Fig. 8 shows voltage and current relationship at no-load versus speed for different capacitor values.

C. Steady state analysis for inductive load

The inductive load is represented by transforming (Z_{Le}) into equivalent R_eC_e shown in Fig. 9 circuit. It is seen that:

$$\left\{\begin{array}{l} R_e = R_L + \dfrac{\omega^2L^2}{4R_L} \\ C_e = C - \dfrac{L}{R_L^2 + \dfrac{\omega^2L^2}{4}} \end{array}\right\} \qquad (34)$$

With the equivalent transformed impedance, the analysis will be similar to that of section A. Fig. 10 shows voltage and load current relationship for different power factors.

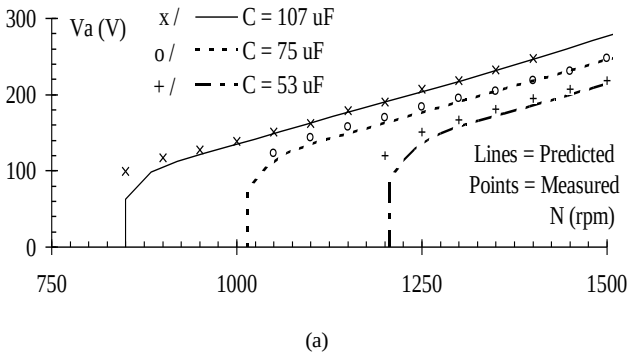

(a)

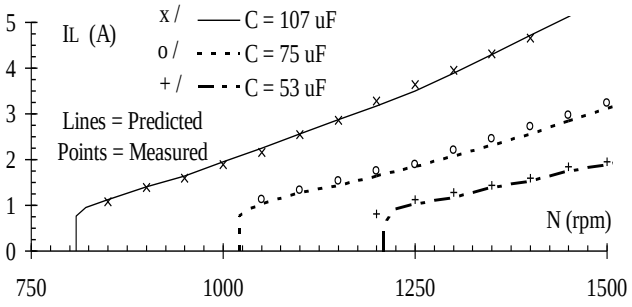

(b)

Fig. 8 Relationship between speed and (a) voltage (b) current at no-load

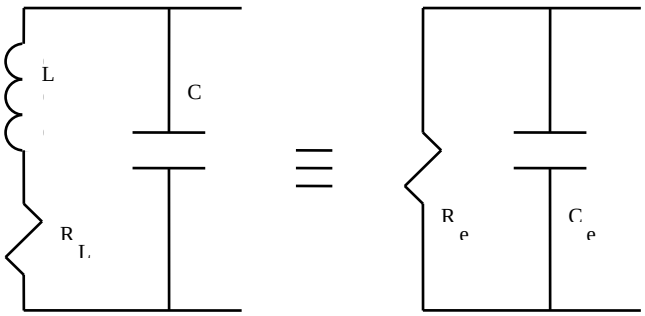

Fig 9. Inductive load transformation

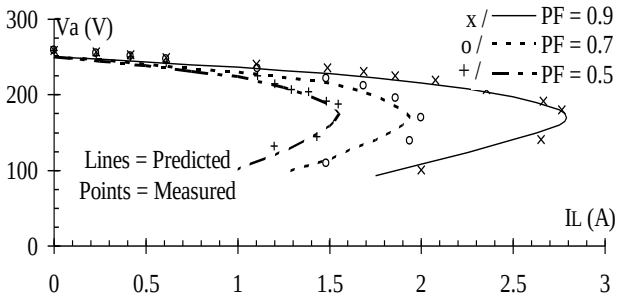

Fig. 10 Phase voltage and load current relationship for inductive load (C=105μF and N = 1400 rpm)

VI. NO-LOAD CAPACITANCE REQUIREMENTS

Similar to induction generator, each speed has a minimum excitation capacitor before which self excitation fails. Self excitation failure occurs when M equals the unsaturated value at point (O) of Fig. 5. With reference to (18), at steady state (PV_q), (PV_d), (PI_q) and (PI_d) equal zero and neither (Vq),(Vd), (Iq) nor (Id) equals zero.

Thus, at point(O), (18) tends to:

$$\begin{vmatrix} -R & \frac{-\omega L_{qo}}{2} & 1 & 0 \\ \frac{\omega L_{do}}{2} & -R & 0 & 1 \\ \frac{-1}{C_{min}} & 0 & 0 & \frac{-\omega}{2} \\ 0 & \frac{-1}{C_{min}} & \frac{\omega}{2} & 0 \end{vmatrix} = 0 \qquad (35)$$

where (L_{do}) and (L_{qo}) are d-q inductances at point (O). Rearranging (35) to get:

$$C_{min} = \frac{2\left(L_{qo}+L_{do}\right)+2\sqrt{\left(L_{do}+L_{qo}\right)^2-\left(\frac{4R}{\omega}\right)^2-4L_{qo}L_{do}}}{4R^2+\omega^2 L_{do}L_{qo}} \qquad .\ .....(36)$$

At point (O):

i_{mo} = 2 A, M_o = 0.287 H, L_{qo} = 0.038 H and L_{do} = 1.838 H

Fig. 11 shows the relation between C_{min} and N.

VII. CONCLUSION

Generalized machine theory was applied for SCSG and d-q model was presented. The model introduced machine, saturation and load representations. D-Q model evaluates performance at transient and steady state. Self-excitation voltage build up has been introduced. Experimental results showed that building up time is short. This could be attributed to the low operating frequency. With an adequate assumption for initial conditions, calculated and measured results show validity of the model to analyze transient state. Steady state analysis is evaluated for resistive, inductive and no-load cases. Calculated and measured results ensure validity of d-q model for steady state analysis as well. The minimum capacitor value to cause self-excitation for a particular speed was calculated.

IX. APPENDIX (A): LOAD TRANSFORMATION

Considering the notation:

$$\left[X_{abc}\right]=\left[X_a \quad X_b \quad X_c\right]^T \qquad (A.1)$$

and

$$\left[X_{dq}\right]=\left[X_d \quad X_q\right]^T \qquad (A.2)$$

As in [8], the relationship between d-q and phase voltages can be written as follows:

$$\left[V_{dq}\right]=\left[A\right]\left[V_{abc}\right] \qquad (A.3)$$

and,

$$\left[V_{abc}\right]=\left[B\right]\left[V_{dq}\right] \qquad (A.4)$$

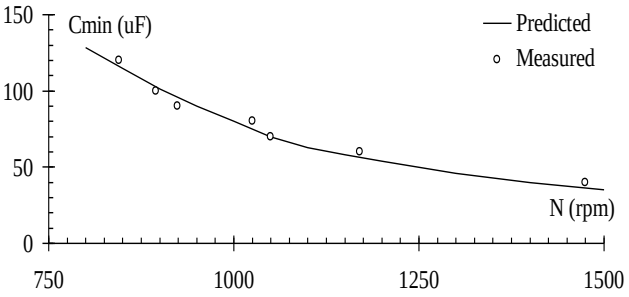

Fig.11 Minimum capacitance and speed relationship

where,

$$\left[A\right]=\frac{2}{3}\begin{bmatrix} \cos(\theta) & \cos\left(\theta-\frac{2\pi}{3}\right) & \cos\left(\theta+\frac{2\pi}{3}\right) \\ \sin(\theta) & \sin\left(\theta-\frac{2\pi}{3}\right) & \sin\left(\theta+\frac{2\pi}{3}\right) \end{bmatrix} \qquad (A.5)$$

and

$$\left[B\right]=\begin{bmatrix} \cos(\theta) & \sin(\theta) \\ \cos\left(\theta-\frac{2\pi}{3}\right) & \sin\left(\theta-\frac{2\pi}{3}\right) \\ \cos\left(\theta+\frac{2\pi}{3}\right) & \sin\left(\theta+\frac{2\pi}{3}\right) \end{bmatrix} \qquad (A.6)$$

The machine model was derived for motor operation. To simulate generator case, phase currents and voltages relationship is given by:

$$\left[V_{abc}\right]=-Z_{Le}\left[i_{abc}\right] \qquad (A.7)$$

where

$$Z_{Le}=\frac{R_L+LP}{1+R_L CP+LCP^2} \qquad \text{(see Fig. 1)} \qquad (A.8)$$

Substituting (A.8) in (A.7) and rearranging yields:

$$\left[v_{abc}\right]+R_L C\left[P\ v_{abc}\right]+LC\left[P^2\ v_{abc}\right]= -R_L\left[i_{abc}\right]-L\left[P\ i_{abc}\right] \qquad (A.9)$$

To get [Pv_{abc}], (A.4) is differentiated w.r.t. time as follows:

$$\left[P\ v_{abc}\right]=\left[PB\right]\left[v_{dq}\right]+\left[B\right]\left[P\ v_{dq}\right] \qquad (A.10)$$

where,

$$\left[B\right]=\left(P\theta\right)\begin{bmatrix} -\sin(\theta) & \cos(\theta) \\ -\sin\left(\theta-\frac{2\pi}{3}\right) & \cos\left(\theta-\frac{2\pi}{3}\right) \\ -\sin\left(\theta+\frac{2\pi}{3}\right) & \cos\left(\theta+\frac{2\pi}{3}\right) \end{bmatrix} \qquad (A.11)$$

Similarly,

$$\left[P\ i_{abc}\right]=\left[PB\right]\left[i_{dq}\right]+\left[B\right]\left[P\ i_{dq}\right] \qquad (A.12)$$

Differentiating (A.10) w.r.t time yields:

$$\left[P^2\ v_{abc}\right]=\left[P^2\ B\right]\left[v_{dq}\right]+2\left[PB\right]\left[P\ v_{dq}\right]+\left[B\right]\left[P^2\ v_{dq}\right] \qquad (A.13)$$

where,

$$\left[P^2\ B\right]=-(P\theta)^2\left[B\right]+\frac{P^2\theta}{P\theta}\left[PB\right] \qquad (A.14)$$

Substituting (A.4), (A.10), (A12), (A.13) and (A.14) in (A.9) yields:

$$\begin{aligned}&\left[B\right]\left[v_{dq}\right]+R_LC\left[PB\right]\left[v_{dq}\right]+R_LC\left[B\right]\left[P\ v_{dq}\right]+LC\frac{P^2\theta}{P\theta}\\&\left[PB\right]\left[v_{dq}\right]-LC(P\theta)^2\left[B\right]\left[v_{dq}\right]+2LC\left[PB\right]\left[P\ v_{dq}\right]+\\&LC\left[B\right]\left[P^2\ v_{dq}\right]=-R_L\left[B\right]\left[i_{dq}\right]-L\left[PB\right]\left[i_{dq}\right]-L\left[B\right]\left[P\ i_{dq}\right]\end{aligned} \qquad (A.15)$$

Multiplying both sides by [A], keeping in mind that [A][B]=[I] (unity matrix) and naming [A][PB] as [D] yields:

$$\begin{aligned}&\left(\left(1-LC(P\theta)^2\right)\left[I\right]+\left(R_LC+LC\frac{P^2\theta}{P\theta}\right)\left[D\right]\right)\left[v_{dq}\right]+\\&\left(R_LC\left[I\right]+2LC\left[D\right]\right)\left[P\ v_{dq}\right]+LC\left[B\right]\left[P^2\ v_{dq}\right]=\\&\left(-R_L\left[I\right]-L\left[D\right]\right)\left[i_{dq}\right]-L\left[P\ i_{dq}\right]\end{aligned} \qquad (A.16)$$

where,

$$\left[D\right]=\left[A\right]\left[PB\right]=P\theta\begin{bmatrix}0 & 1\\ -1 & 0\end{bmatrix} \qquad (A.17)$$

If the speed is assumed constant, thus

$$\left\{P\theta=\frac{\omega}{2}\ ,\ P^2\theta=0\right\} \qquad (A18)$$

Substituting by (A.17) and (A.18) into (A.16) and rearranging results in (14).

X. REFERENCES

[1] E.D. Bassett and F.M. Potter, "Capacitive excitation for induction generators," AIEE Trans., May 1935, pp. 540-545.

[2] C.F. Wagner, "Self excitation of induction motors," AIEE Trans., vol. 58, Feb. 1939, pp. 47-51.

[3] I.R. Smith and S. Sriharan, "Transient in induction machines with terminal capacitors," Proc. IEE, vol. 115, no. 4, April 1968.

[4] S.S. Murthy, O.P. Malik and K. Tandon, "Analysis of self-excited generators," IEE Proc., vol. 129, no. 6, Nov. 1982, pp. 360-365.

[5] A.S. Mostafa, A.L. Mohamadein and E.M. Rashad, "Analysis of series connected wound rotor self excited induction generator," IEE Proc. B, Vol. 140, No. 5, Sept 1993.

[6] A.S. Mostafa, A.L. Mohamadein and E.M. Rashad, "Application of Floquet's theory to the analysis of series-connected wound-rotor self-excited synchronous generator," IEEE Trans. on EC, Vol. 8, No. 3, Sept. 1993.

[7] A.L. Mohamadein and E.A Shehata, "Theory and performance of series connected self excited synchronous generator," IEEE Trans. on EC, Vol. 10, No. 3, Sept. 1995.

[8] P.C. Krause and C.H. Thomas, "Simulation of symmetrical induction machinery," IEEE Trans. PAS, vol. 84, no. 11, Nov. 1965, pp. 1038-1053.

XI. BIOGRAPHIES

Prof. Adel L. Mohamadein (SM'83) was born in Alexandria in Dec. 1947. He obtained his BSc and MSc from Alexandria University in 1968 and 1971 respectively and his PhD from UMIST in 1974. He is an IEE member. Prof. Mohamadein is now the Vice Dean for Graduate Studies and Research in the College of Engineering, Alexandria University. He has been delegated to King Saud University twice in the area of Electrical Machines, Drives and Power Electronics where he has published around 60 papers.

Hassan Yousef graduated from Alexandria University in 1979. He obtained his PhD degree from Pennsylvania, USA. He is now an associate Professor in Qatar University. His interest involves adaptive and optimal control techniques.

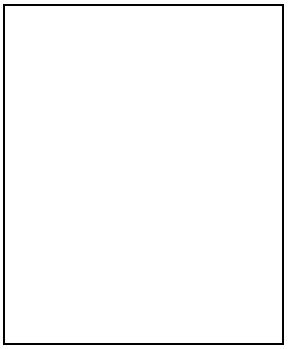

Yasser Gaber Dessouky was born in 1969, Alexandria, Egypt. He received BSc and MSc degrees in 1991 and 1993 respectively from Alexandria University, Egypt. He got his PhD from Heriot-Watt University, Edinburgh, UK in 1998. He is currently a lecturer in the Arab Academy for Science and Technology, Alexandria, Egypt. His interest involves power electronics, machine drives and microprocessor controlled systems.